or strong C–C/C–H bonds makes an important contribution to the driving force. Although Cp'_2Sm–H and Cp'_2Sm–alkyl bonds are relatively strong, they are insufficiently strong to effectively drive hydrocarbon functionalization by dinuclear oxidative addition processes. The exceptions are hydrocarbons having weak C–H bonds and forming strong metal–ligand bonds (e.g., propylene → η^3-allyl), or cases where a highly exothermic follow-up process can be coupled to C–H scission. Further exploitation of these bond enthalpy trends and extensions to other lanthanides will be the subjects of future contributions.

Acknowledgment. We are grateful to NSF for support of this research under Grant CHE8800813. D.S. thanks Rhône-Poulenc for a fellowship. We thank W. R. Grace for gifts of dessicants.

Registry No. 1, 90866-66-3; **2**, 122213-83-6; **3**, 122213-84-7; **4**, 122213-85-8; **5**, 79372-14-8; **6**, 103933-62-6; **7**, 84751-30-4; **8**, 98720-37-7; **9**, 122213-86-9; **10**, 122213-87-0; **11**, 122213-88-1; **12**, 108394-59-8; **13**, 122213-89-2; **14**, 122213-90-5; **15**, 122213-91-6; $CH_3CH{=}CH_2$, 115-07-1; $HNMe_2$, 124-40-3; $(t\text{-Bu})_2CHOH$, 14609-79-1; $n\text{-}C_5H_{11}Cl$, 543-59-9; $n\text{-}C_4H_9Br$, 109-65-9; HS^nPr, 107-03-9; $HPEt_2$, 627-49-6; HCCPh, 536-74-3.

Ferromagnetically Coupled Linear Electron-Transfer Complexes. Structural and Magnetic Characterization of $[Cr(\eta^6\text{-}C_6Me_xH_{6-x})_2][TCNE]$ (x = 0, 3, 6) and S = 0 $[TCNE]_2^{2-}$

Joel S. Miller,*[1a] Dermot M. O'Hare,[1a,b] Animesh Chakraborty,[1c] and Arthur J. Epstein*[1c]

Contribution No. 5045 from Central Research and Development Department, E. I. du Pont de Nemours and Co., Inc., Experimental Station E328, Wilmington, Delaware 19880-0328, and Department of Physics and Department of Chemistry, The Ohio State University, Columbus, Ohio 43210. *Received March 3, 1989*

Abstract: The reaction of $Cr^0(C_6Me_xH_{6-x})_2$ (x = 0, 3, 6), D, with TCNE, A, results in formation of 1:1 electron-transfer salts of $[Cr^I(C_6Me_xH_{6-x})_2][TCNE]$ (x = 0, 3, 6) composition. The x = 0 and 3 complexes have been structurally characterized. The $[Cr^I(C_6H_6)_2]^{\bullet+}$ salt belongs to the centrosymmetric $P2_1/m$ space group [a = 10.347 (4) Å, b = 12.423 (10) Å, c = 12.763 (4) Å, β = 111.33 (3)°, Z = 4, T = 23 °C, V = 1528 (3) Å^3, R_u = 0.042, and R_w = 0.044]. The $[TCNE]^{\bullet-}$ anion has average C–C, C–CN, and C≡N bonds of 1.436, 1.414, and 1.140 Å, respectively, and the NC–C–CN, NC–C–C, and N≡C—C angles average 118.6, 120.2, and 178.4°, respectively. The solid-state structure consists of linear chains of $\cdots D^{\bullet+}A_2^{2-}D^{\bullet+}D^{\bullet+}A_2^{2-}D^{\bullet+}\cdots$ with the anion existing as dimeric dianions, $[TCNE]_2^{2-}$. The $[TCNE]_2^{2-}$ is centrosymmetric, and the intradimer C···C bond distance is 2.904 Å. The S = 0 $[TCNE]_2^{2-}$ dimer is nonplanar and bent 10° via a b_{3u} out-of-plane distortion. One habit of the $[Cr(C_6Me_3H_3)_2]^{\bullet+}$ salt crystallizes in the $P\bar{1}$ space group [a = 10.475 (5) Å, b = 11.427 (4) Å, c = 8.419 (6) Å, α = 64.20 (3)°, β = 78.59 (4)°, γ = 81.56 (3)°, Z = 2, T = 23 °C, V = 1266 (9) Å^3, R_u = 0.075, and R_w = 0.081]. This is a poorer quality structure with average C–C, C–CN, and C≡N bonds of 1.45, 1.40, and 1.10 Å, respectively, while the NC–C–CN, NC–C–C, and N≡C—C angles average 133, 114, and 162°, respectively. The solid-state structure also consists of linear chains of $\cdots D^{\bullet+}A_2^{2-}D^{\bullet+}D^{\bullet+}A_2^{2-}D^{\bullet+}\cdots$ with the intradimer separation of 3.09 Å for the $[TCNE]_2^{2-}$. The $[TCNE]_2^{2-}$ dimer exhibits three characteristic C≡N vibrations in the infrared region at 2160 s, 2169 s, and 2190 m cm^{-1}. The $[Cr^I(C_6H_6)_2]^{\bullet+}$ and this $[Cr^I(C_6Me_3H_3)_2]^{\bullet+}$ structure have eclipsed and staggered conformations, respectively. The average Cr–C and C–C separations are 2.143 and 1.395 Å, respectively, for $[Cr^I(C_6H_6)_2]^{\bullet+}$, and the average Cr–C, C–C, and C–Me separations for $[Cr^I(C_6Me_3H_3)_2]^{\bullet+}$ are 2.16, 1.40, and 1.51 Å, respectively. The Cr–C_6(ring) centroids are equivalent at 1.625 (5) Å. The magnetic susceptibility between 2 and 320 K for these $[TCNE]_2^{2-}$ complexes can be fit by the Curie–Weiss law, $\chi = C/(T - \theta)$, for one independent per spin repeat unit. In solution two signals with g = 2.001 and 1.896 characteristic of $[TCNE]^{\bullet-}$ and $[Cr(\eta\text{-arene})_2]^{\bullet+}$ are observed; thus, $[TCNE]^{\bullet-}$ and not $[TCNE]_2^{2-}$ is present in solution. For the solid phase the spin is assigned to the cation; with the dimer being diamagnetic. A second structure type is suggested for the $[Cr^I(C_6Me_xH_{6-x})_2]^{\bullet+}$ (x = 3, 6) salts as they exhibit the characteristic ν(C≡N) vibrations for an isolated $[TCNE]^{\bullet-}$. Their high-temperature susceptibility can be fit by the Curie–Weiss law with θ = ~+11.4 K and μ_{eff} = ~2.4 μ_B consistent with ferromagnetic coupling; thus, we propose that these complexes possess a $\cdots D^{\bullet+}A^{\bullet-}D^{\bullet+}A^{\bullet-}\cdots$ chain structure. The magnetization saturated faster than accountable by the Brillouin function for independent spins; however, bulk 3-D ordering is not evident. The configurational mixing of a charge-transfer excited state with the ground-state model predicts antiferromagnetic coupling should be stabilized for this compound as both the donor and acceptor possess an $^2A_{1g}$ ground state. Charge-transfer excitation from the next highest occupied molecular orbital, however, is consistent with the stabilization of ferromagnetic coupling for this system. Thus, other molecular/organic systems with ^2A ground states might be suitable components for a bulk ferromagnet.

One-dimensional, 1-D, electron-transfer complexes have been frequently characterized to exhibit unusual optical and electrical[2-4] and recently unusual cooperative magnetic properties.[5] For example, the reaction of decamethylferrocene, $Fe(C_5Me_5)_2$, and

(1) (a) du Pont. (b) Current address: Oxford University. (c) Ohio State University.

(2) See for example: *Extended Linear Chain Compounds*; Miller, J. S., Ed.; Plenum: New York; 1982, Vol. 1, 2; 1983, Vol. 3. Simon, J.; Andre, J. J. *Molecular Semiconductors*, Springer-Verlag: New York, 1985.

(3) For detailed overview, see the proceedings of the recent series of international conferences: *Synth. Met.* **1987**, 17–19. *Mol. Cryst. Liq. Cryst.* **1985**, 117–121. *J. Phys. (Paris) Coll.* **1983**, 44–C3. *Mol. Cryst. Liq. Cryst.* **1981**, *77*, *79*, *82*, *83*, *85*, *86*, **1982**. *Chem. Scr.* **1981**, *17*. *Lect. Notes Phys.* **1979**, *95*, *96*. *Ann. N.Y. Acad. Sci.* **1978**, 313.

0002-7863/89/1511-7853$01.50/0

7,7,8,8-tetracyano-*p*-quinodimethane, TCNQ, gives three major products of varying stoichiometry, conductivity, and magnetism. Two 1:1 electron-transfer salts can be isolated.[6] The kinetic phase is comprised of a 1-D structural motif based on alternating $S = {}^1/_2$ $[Fe(C_5Me_5)_2]^{\bullet+}$ cation donors, D, and $S = {}^1/_2$ $[TCNQ]^{\bullet-}$ anion acceptors, A, i.e., $\cdots D^{\bullet+}A^{\bullet-}D^{\bullet+}A^{\bullet-}\cdots$, and has been reported to have a field-dependent metamagnetic switching from an antiferromagnetic to a high moment behavior.[5,7] Molecular metamagnetic materials are of fundamental interest; however, the lack of large single crystals and low transition temperature have hampered the detailed study of physical properties. Replacement of $[TCNQ]^{\bullet-}$ with $[TCNE]^{\bullet-}$ (TCNE = tetracyanoethylene) has lead to the similarly structured $[Fe(C_5Me_5)_2]^{\bullet+}[TCNE]^{\bullet-}$, which has been characterized to be a bulk ferromagnet.[5,8,9]

With our observation of ferro- and metamagnetic behavior in 1-D molecular electron-transfer complexes, we purposely sought to elucidate the structure–function relationships by modification of the radical cation and independently the radical anion.[5] We were attracted to the isoelectronic group 6A d^5 bisarene cations for direct comparison to the highly magnetic $[Fe(C_5Me_5)_2]^{\bullet+}$-based electron-transfer complexes and preparation of new meta- and ferromagnetic substances with higher transition temperatures.

Bis(benzene)chromium[11,12] and bis(toluene)chromium[11,13-15] have been reported to form 1:1[11-13] and 1:2[11,14,15] electron-transfer salts with TCNQ. The X-ray structure of the 1:1 salt with bis(toluene)chromium has been determined[13] and consists of segregated stacks of cations and anions. The magnetic susceptibility of $[Cr(C_6H_6)_2][TCNQ]$ and $[Cr(C_6H_5Me)_2][TCNQ]$ is consistent with only one unpaired electron per repeat unit. The spin is assigned to the Cr^I cation.[11] We were interested in preparing TCNE charge-transfer salts of [bis(arene)chromium]$^{\bullet+}$ with a view to preparing new low-dimensional magnetic materials. The initially selected radical anions were $[TCNE]^{\bullet-}$ and $[TCNQ]^{\bullet-}$.[10]

The best conceptual framework to view the stabilization of ferromagnetic coupling in molecular based donor/acceptor complexes is based upon the extended[17] McConnell mechanism.[16] Within this model, the stabilization of ferromagnetic coupling arises from the configurational mixing of a charge-transfer excited state with the ground state.[5,16,17] The model predicts that for excitation from the HOMO of a donor with a half-filled HOMO {as is the case for $[Cr(arene)_2]^{\bullet+}$} to an acceptor with a half-filled nondegenerate HOMO {as is the case from $[TCNE]^{\bullet-}$}, only antiferromagnetic coupling is stabilized. Thus, the radical anion electron-transfer salts of $[Cr(C_6H_xMe_{6-x})_2]^{\bullet+}$ and $[TCNE]^{\bullet-}$ provide a means to test these concepts. Thus, herein we report complexes based on $[Cr(C_6H_xMe_{6-x})_2]^{\bullet+}$ and $[TCNE]^{\bullet-}$.

Table I. Crystallographic Parameters for $[Cr(C_6H_6)_2][TCNE]$, **1**

formula	$C_{18}H_{12}N_4Cr$
formula mass	336.32
space group	$P2_1/m$
a, Å	10.347 (4)
b, Å	12.423 (10)
c, Å	12.763 (4)
α, deg	90.0
β, deg	111.33 (3)
γ, deg	90.0
V, Å^3	1528 (3)
Z	4
ρ(calc), g cm^{-3}	1.46
temp, °C	23
radiation	Mo Kα
abs coeff, cm^{-1}	7.3
scan mode	ω–θ
2θ max, deg	48.0
total data measd	2661
unique data with $(F_o)^2 > 3\sigma(F_o)^2$	2160
final no. of variables	217
R_u (F^2)	0.042
R_w (F^2)	0.044
largest residual, e Å^{-3}	0.53 (5)

Experimental Section

All reactions were performed by using standard Schlenk techniques or in a Vacuum Atmospheres Dri-Box under a nitrogen atmosphere. EPR spectra were recorded on an IBM/Bruker ER 200 D-SRC spectrometer. Magnetic susceptibility data were recorded by using the Faraday technique from 2 to 300 K. Infrared spectra were recorded on a Nicolet 7199 Fourier transform spectrometer. Elemental analysis and single-crystal X-ray studies were performed by Oneida Research Services, Inc. (Whitesboro, NY). $[Cr(\eta^6\text{-}C_6Me_xH_{6-x})_2]$ (x = 0, 3, 6),[18a] $Fe(C_5H_4(CH_2)_3)_2$,[19] and $[Fe(C_5H_4(CH_2)_3)_2]^{\bullet+}[TCNE]^{\bullet-}$[20] were prepared according to the literature routes; TCNE (Aldrich) was sublimed prior to use.

$[Cr(\eta^6\text{-}C_6H_6)_2]^{\bullet+}[TCNE]^{\bullet-}$, **1**, was prepared from reaction of $Cr(\eta^6\text{-}C_6H_6)_2$ and TCNE by the method first described by Fitch and Lagowski.[21] Typically $Cr(\eta^6\text{-}C_6H_6)_2$ (100 mg, 0.47 mmol) was dissolved in 10 mL of CH_3CN and added to a solution of TCNE (60.4 mg, 0.47 mmol) in 3–4 mL of CH_3CN. The dark red solution was concentrated to ca. 5 mL. Cooling to −25 °C for 2–3 days produced dark red plates which were collected by vacuum filtration; yield (127 mg, 80%). Anal. Calcd (found) for $C_{18}H_{12}N_4Cr$: C, 64.28 (64.00, 63.98); H, 3.60 (3.55, 3.63); N, 16.66 (16.61, 16.59). Infrared {Nujol, ν(C≡N)} 2159 s, 2170 s, and 2189 m cm^{-1}.

α-$[Cr(\eta^6\text{-}C_6Me_3H_3)_2]^{\bullet+}[TCNE]^{\bullet-}$, 2$\alpha$. $Cr(\eta^6\text{-}C_6Me_3H_3)_2$ (50 mg, 0.17 mmol) was dissolved in 10 mL of THF and added to a solution of TCNE (22 mg, 0.17 mmol) in 3–4 mL of THF. The red solution was concentrated to ca. 5 mL. Cooling to −25 °C overnight produced red-brown crystals which were collected by vacuum filtration; yield (54 mg, 70%). Anal. Calcd (found) for $C_{24}H_{24}N_4Cr$: C, 68.56 (68.72, 68.15); H, 5.75 (5.73, 5.56); N, 13.32 (13.44, 13.16). Infrared {Nujol, ν(C≡N)} 2144 s and 2183 m cm^{-1}.

In addition to these crystals on one occasion cooling of a 30-mL dilute solution overnight to −25 °C produced one large crystal (2 × 5 × 1 mm) of the β-phase, **2β**, which was collected by vacuum filtration. Attempts to reproduce the preparation of the β-phase were unsuccessful, and insufficient amount of the β-phase was available for physical measurements.

$[Cr(\eta^6\text{-}C_6Me_6)_2]^{\bullet+}[TCNE]^{\bullet-}$, 3, was prepared as described above. $Cr(\eta^6\text{-}C_6Me_6)_2$ (100 mg, 0.26 mmol) was dissolved in 10 mL of THF and added to a solution of TCNE (34 mg, 0.26 mmol) in 3–4 mL of THF. The red solution was concentrated to ca. 5 mL. Cooling to −25 °C

(4) Epstein, A. J.; Miller, J. S. *Sci. Am.* **1979**, *241*(4), 52–61. Bechgaard, K.; Jerome, D. *Sci. Am.* **1982**, *247*(2), 52–61.

(5) (a) Miller, J. S.; Epstein, A. J.; Reiff, W. M. *Chem. Rev.* **1988**, *88*, 201–220. (b) Miller, J. S.; Epstein, A. J.; Reiff, W. M. *Isr. J. Chem.* **1987**, *27*, 363–373. Miller, J. S.; Epstein, A. J. *NATO Adv. Studies Ser. B* **1988**, *168*, 159–174. Miller, J. S.; Epstein, A. J.; Reiff, W. M. *Acc. Chem. Res.* **1988**, *21*, 114–120. Miller, J. S.; Epstein, A. J.; Reiff, W. M. *Science* **1988**, *240*, 40–47.

(6) Miller, J. S.; Reiff, W. M.; Zhang, J. H.; Preston, L. D.; Reis, A. H., Jr.; Gebert, E.; Extine, M.; Troup, J.; Dixon, D. A.; Epstein, A. J., Ward, M. D. *J. Phys. Chem.* **1987**, *91*, 4344–4360.

(7) Candela, G. A.; Swartzendruber, L.; Miller, J. S.; Rice, M. J. *J. Am. Chem. Soc.* **1979**, *101*, 2755–2756.

(8) (a) Miller, J. S.; Calabrese, J. C.; Bigelow, R. W.; Epstein, A. J.; Zhang, J. H.; Reiff, W. M. *J. Chem. Soc., Chem. Commun.* **1986**, 1026–1028. (b) Miller, J. S.; Calabrese, J. C.; Rommelmann, H.; Chittapeddi, S.; Zhang, J. H.; Reiff, W. M.; Epstein, A. J. *J. Am. Chem. Soc.* **1987**, *109*, 769–781.

(9) Chittapeddi, S.; Cromack, K. R.; Miller, J. S.; Epstein, A. J. *Phys. Rev. Lett.* **1987**, *22*, 2695.

(10) O'Hare, D. M.; Ward, M. D.; Miller, J. S., manuscript in preparation.

(11) Zvarykina, A. V.; Karimov, Yu. S.; Ljubovsky, R. B.; Makova, M. K.; Khidekel, M. L.; Shchogelov, I. F.; Yagubsky, E. B. *Mol. Cryst. Liq. Cryst.* **1970**, *11*, 217–228.

(12) Yagubskii, E. B.; Khidekel, M. L.; Shchogelov, I. F.; Buravov, L. I.; Gribov, B. G.; Makova, M. K. *Dokl. Akad. Nauk. SSSR Ser. Khim.* **1968**, 2013–2014.

(13) Shibaeva, R. P.; Atovmyan, L. O.; Rozenberg, L. P. *J. Chem. Soc., Chem. Commun.* **1969**, 649–650.

(14) (a) Shibaeva, R. P.; Atovmyan, L. O.; Orfanova, M. N. *J. Chem. Soc., Chem. Commun.* **1969**, 1494. (b) Shibaeva, R. P.; Atovmyan, L. O.; Ponomarev, V. I. *J. Struct. Chem.* **1978**, *16*, 792–795.

(15) Ljubovsky, R. B.; Makova, M. K.; Khidekel, M. L.; Shchogelov, I. F.; Yagubskii, E. B. *Zh. Eksp. Teor. Fiz., Pis'ma Red.* **1972**, *15*, 65–659.

(16) McConnell, H. M. *Proc. R. A. Welch Found. Chem. Res.* **1967**, *11*, 144.

(17) Miller, J. S.; Epstein, A. J. *J. Am. Chem. Soc.* **1987**, *109*, 3850–3855.

(18) (a) Anderson, S. E.; Drago, R. S. *J. Am. Chem. Soc.* **1970**, *92*, 4244. (b) Anderson, S. E.; Drago, R. S. *Inorg. Chem.* **1972**, *11*, 3564.

(19) Reinhart, K. L., Jr.; Curby, R. J., Jr.; Gustafson, D. H.; Harrison, K. G.; Bozak, R. E.; Bublitz, D. E. *J. Am. Chem. Soc.* **1962**, *84*, 3263.

(20) Lemervoskii, D. A.; Stukan, R. A.; Tarasevich, B. N.; Slovokhotov, Yu. L.; Antipin, M. Yu.; Kalinin, A. E.; Struchov, Yu. T. *Struct. Khim.* **1981**, *7*, 240.

(21) Fitch, J. W., III; Lagowski, J. J. *Inorg. Chem.* **1965**, *4*, 864–867.

Table II. Bond Distances for $[Cr(C_6H_6)_2]^{\bullet+}[TCNE]^{\bullet-}$, **1**[a]

at. 1	at. 2	dist, Å	at. 1	at. 2	dist, Å
Cr(1)	C(1)	2.154 (5)	C(1)	C(2)	1.384 (5)
C(13)	C(13)	1.424 (6)	Cr(1)	C(2)	2.147 (4)
Cr(1)	C(3)	2.137 (4)	C(2)	C(3)	1.398 (7)
C(15)	C(15)	1.441 (6)	Cr(1)	C(4)	2.144 (6)
C(15)	C(16)	1.377 (7)	Cr(1)	C(5)	2.137 (5)
C(3)	C(4)	1.394 (6)	Cr(1)	C(6)	2.143 (4)
C(16)	C(17)	1.382 (7)	Cr(1)	C(7)	2.145 (4)
Cr(1)	C(8)	2.135 (6)	C(5)	C(6)	1.394 (6)
C(17)	C(17)	1.366 (6)	Cr(2)	C(11)	2.151 (4)
Cr(2)	C(12)	2.146 (4)	C(6)	C(7)	1.391 (7)
C(18)	C(20)	1.408 (5)	Cr(2)	C(13)	2.138 (3)
C(17)	C(17)	1.366 (6)	Cr(2)	C(15)	2.133 (4)
C(7)	C(8)	1.391 (6)	C(18)	C(20)	1.408 (5)
Cr(1)	C(16)	2.144 (4)	C(19)	C(20)	1.423 (5)
Cr(2)	C(17)	2.153 (3)	C(20)	C(20)	1.436 (5)
N(18)	C(18)	1.136 (6)	C(11)	C(11)	1.417 (6)
C(21)	C(23)	1.419 (5)	N(19)	C(19)	1.145 (6)
C(11)	C(12)	1.379 (6)	C(22)	C(23)	1.408 (5)
N(21)	C(21)	1.138 (5)	C(23)	C(23)	1.436 (5)
N(22)	C(22)	1.140 (5)			

[a] Numbers in parentheses are estimated standard deviations in the least significant digits.

overnight produced dark red plates which were collected by vacuum filtration; yield (98 mg, 75%). Anal. Calcd (found) for $C_{38}H_{36}N_4Cr$: C, 71.40 (70.98); H, 7.19 (7.09); N, 11.10 (10.54). Infrared {Nujol, $\nu(C\equiv N)$} 2144 and 2183 cm^{-1}.

X-ray Structure Determination. X-ray Data Collection. $[Cr(C_6H_6)_2]^{\bullet+}[TCNE]^{\bullet-}$, **1**, crystals were grown by slow cooling of a saturated acetonitrile solution. Crystallographic details are presented in Table I. Cell constants and an orientation matrix for the data collection were obtained from least-squares refinement using the angles of 25 reflections in the range $12 < \theta < 20°$. Systematic absences and subsequent least-squares refinement determined the space group to be $P2_1/m$. During data collection the intensity of three representative reflections were measured as a check on crystal stability. There was loss of intensity during data collection, and an isotropic decay correction was applied. The correction factors on I ranged from 0.992 to 1.206. Equivalent reflections were merged, and only those for which $(F_o)^2 > 3\sigma(F_o)^2$ were included in the refinement where $\sigma(F_o)^2$ is the standard deviation based on counting statistics. Data were also corrected for Lorentz and polarization factors. No absorption correction was made.

$[Cr(C_6Me_3H_3)_2]^{\bullet+}[TCNE]^{\bullet-}\cdot MeCN$, **2β**, crystallizes in the $P\bar{1}$ triclinic space group and is a poorer quality structure by conventional crystallographic standards. In addition the 1-D $\cdots D^{\bullet+}D^{\bullet+}A_2^{2-}\cdots$ motif is similar (vide infra) to **1**, and thus we present the structure as supplementary material (see the paragraph at the end of the paper).

Structure Solution and Refinement. $[Cr(C_6H_6)_2]^{\bullet+}[TCNE]^{\bullet-}$, **1.** The structure was solved by direct methods. Two atoms were located from an E map prepared from the phase set with probability statistics. The two cations were bisected by a mirror at $y = {}^1/_4$, and the remaining atoms were located in succeeding difference Fourier syntheses. Hydrogen atoms were added to the structure factor calculations at their calculated positions, but their positions were not refined.

Neutral atom scattering factors were taken from Cromer and Waber.[22] Anomalous dispersion effects were included in F_c;[23] the values for f' and f'' were those from the literature.[24] All calculations were performed on a VAX-11/750 computer using the SDP-PLUS package.[25]

$[Cr(C_6Me_3H_3)_2]^{\bullet+}[TCNE]^{\bullet-}\cdot MeCN$, 2β. The structure was solved by direct methods. One atom was located from an E map prepared from the phase set with probability statistics, and the remaining atoms were located in succeeding difference Fourier syntheses. The $[TCNE]^-$ anion was poorly resolved in the Fourier syntheses; as a consequence the internal ethylenic carbons were held at fixed idealized positions, and the cyano groups were independently refined. Larger than expected thermal parameters were calculated for C(40) and C(42). Hydrogen atoms were added to the structure factor calculations at their calculated positions, but their positions were not refined. Neutral atom scattering factors, anomalous dispersion effects, and the values for f' and f'' were determined and all calculations were carried out as described above.

Table III. Anion Bond Angles for $[Cr(C_6H_6)_2]^{\bullet+}[TCNE]^{\bullet-}$, **1**[a]

at. 1	at. 2	at. 3	angle, deg	at. 1	at. 2	at. 3	angle, deg
N(22)	C(22)	C(23)	177.9 (4)	N(18)	C(18)	C(20)	178.1 (4)
C(21)	C(23)	C(22)	118.8 (3)	N(21)	C(21)	C(23)	178.6 (4)
C(21)	C(23)	C(23)	120.5 (3)	N(19)	C(19)	C(20)	179.1 (4)
C(18)	C(20)	C(19)	118.3 (3)	C(19)	C(20)	C(20)	120.6 (3)
C(22)	C(23)	C(23)	119.8 (3)	C(18)	C(20)	C(20)	119.7 (3)

[a] Numbers in parentheses are estimated standard deviations in the least significant digits.

Table IV. Dihedral Angles between Planes[a] for $[Cr(\eta^6\text{-}C_6H_6)_2]^{\bullet+}[TCNE]^{\bullet-}$, **1**

plane no.	plane no.	dihedral angle, deg
1[b]	2[c]	3.33 ± 2.38
1	3[d]	12.40 ± 0.55
1	4[e]	9.48 ± 0.68
2	3	12.56 ± 0.57
2	4	8.98 ± 0.75
3	4	21.42 ± 0.23

[a] The deviation of each atom within the least-squares plane is within experimental error. [b] Plane 1: C1, C2, C3, C4. [c] Plane 2: C5, C6, C7, C8. [d] Plane 3: N18, N19, C18, C19, C20. [e] Plane 4: N21, N22, C21, C22, C23.

Results and Discussion

Chemistry. The reaction of TCNE with metallocenes can result in a variety of 1:1 products with different structural motifs.[5] The bisarene transition-metal complexes, although of different symmetry, are also electron rich and can be readily oxidized[18a] by organic cyano acceptors such as TCNE. Reaction of bis(arene)chromium complexes with a stoichiometric amount of TCNE in acetonitrile results in spontaneous electron transfer giving solutions containing $[Cr(\eta^6\text{-arene})_2]^{\bullet+}[TCNE]^{\bullet-}$. Slow crystallization of solutions from acetonitrile solution yields X-ray-quality crystals, and the structures of $[Cr(\eta\text{-}C_6H_6)_2]^{\bullet+}[TCNE]^-$, **1**, and $[Cr(\eta\text{-}C_6Me_3H_3)_2]^{\bullet+}[TCNE]^{\bullet-}\cdot MeCN$, **2β**, have been determined. Crystals of **2β** rapidly lose the MeCN solvent of crystallization, and crystals had to be placed in epoxy resin to obtain its structure. Crystals of **2α** and **3** grown from THF or CH_2Cl_2/diethyl ether were unsuitable for X-ray diffraction studies but exhibit ferromagnetic ordering at low temperatures (vide infra). Crystalline samples of **1** obtained from THF are not single-phase materials.

Crystal Structures of $[Cr(C_6H_6)_2]^{\bullet+}[TCNE]^{\bullet-}$, 1, and $[Cr(C_6Me_3H_3)_2]^{\bullet+}[TCNE]^{\bullet-}\cdot MeCN$, 2β. Compound **1** crystallizes in the monoclinic $P2_1/m$ space group. The atom labeling and bond distances for $[Cr(C_6H_6)_2]^{\bullet+}[TCNE]^-$ can be found in Figure 1 and Table II, respectively. The anion bond angles and least-squares planes are given in Tables III and IV. Tables of positional coordinates, thermal parameters, and cation bond angles are found in Tables S1–S3 (supplementary material), respectively. As discussed earlier, **2β** is a poorer quality structure with a motif similar to **1** and is presented as supplementary material.

The $[Cr^I(C_6H_6)_2]^{\bullet+}$ cation in **1** is a well-resolved ordered D_{6h} ion possessing distances essentially equivalent to those previously reported for this cation as the $[TCNQ]^-$ or I^- salts.[26,27] The Cr–C and C–C distances range from 2.133 (4) to 2.154 (5) and 1.366 (6) to 1.441 (6) Å and average 2.143 and 1.395 Å, respectively. The Cr–C_6(ring) centroid is 1.62 (1) Å. The $[Cr^I(C_6Me_3H_3)_2]^{\bullet+}$ cation in **2β** is in a staggered conformation with distances essentially equivalent to those in **1**. The Cr–C, C–C, and C–Me separations range from 2.14 (1) to 2.19 (2), 1.35 (2) to 1.47 (3), and 1.47 (3) to 1.54 (2) Å and average 2.16, 1.40, and 1.51 Å,

(22) Cromer, D. T.; Waber, J. T. *International Tables for X-Ray Crystallography*; The Kynoch Press: Birmingham, England, 1974; Vol. IV, Table 2.2B.

(23) Ibers, J. A.; Hamilton, W. C. *Acta Crystallogr.* **1964**, *17*, 781.

(24) Cromer, D. T.; Waber, J. T. *International Tables for X-Ray Crystallography*; The Kynoch Press: Birmingham, England, 1974; Vol. IV, Table 2.3.1.

(25) Frenz, B. A. The Enraf-Nonius CAD 4 SDP-A Real Time System for Concurrent X-Ray Data Collection and Crystal Structure Determination. In *Computing in Crystallography*; Schenk, H., Olthof-Hazelkamp, R., Vankonigsveld, H., Bassi, G. C., Eds.; Delft University Press: Holland, 1978; pp 64–71.

(26) Shibaeva, R. P.; Shvets, A. E.; Atovmyan, L. O. *Dokl. Akad. Nauk. SSSR* **1971**, *199*, 334.

(27) Morosin, B. *Acta. Crystallogr., Sect. B* **1974**, *30*, 838.

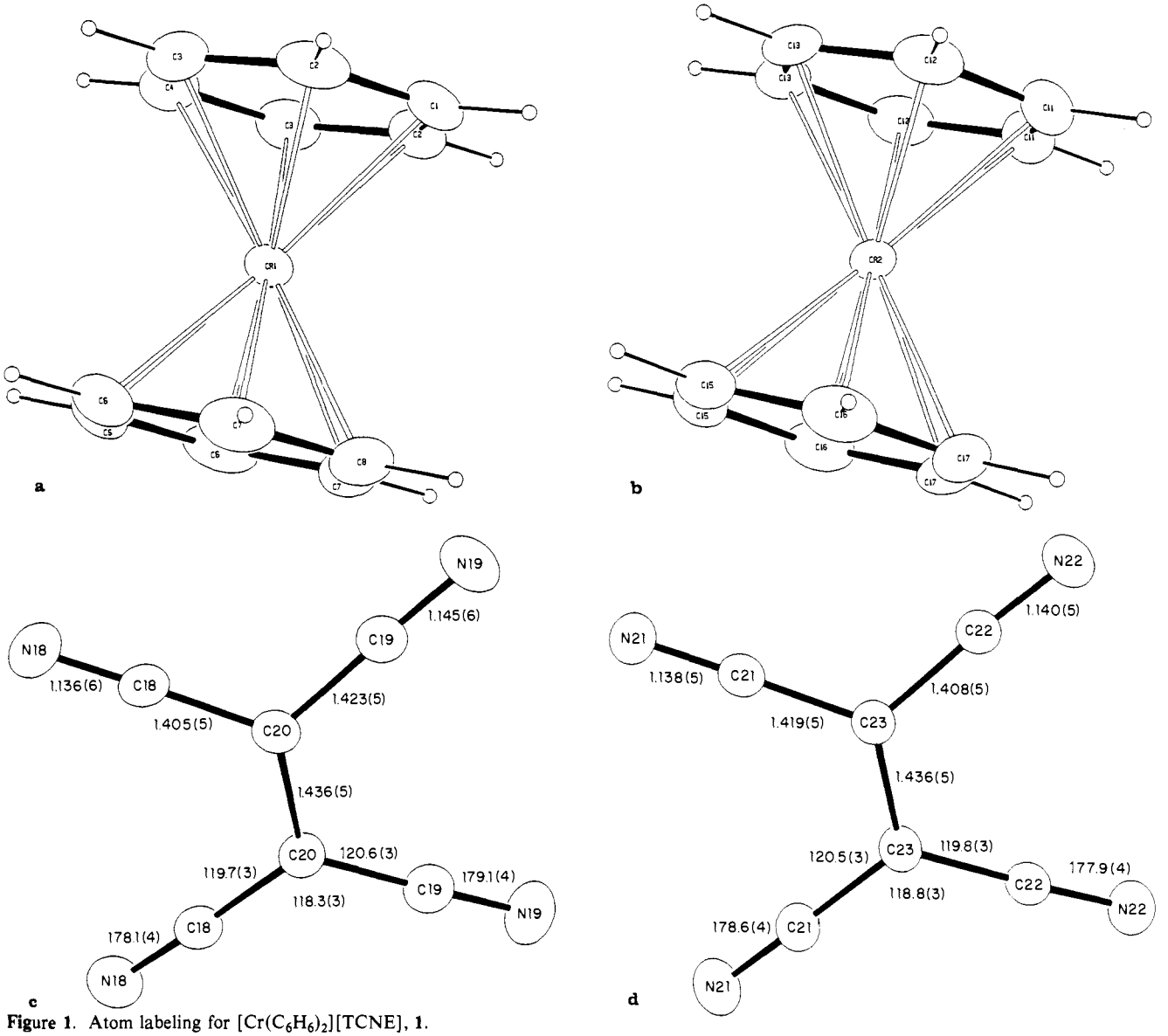

Figure 1. Atom labeling for $[Cr(C_6H_6)_2][TCNE]$, **1**.

respectively. The Cr–C_6(ring) centroid distance is 1.63 (1) Å.

These intracation Cr–C and C–C distances are essentially equivalent: the values of 2.141_5 and 1.416_5 Å obtained for Cr-$(C_6H_6)_2$ at 100 K,[28] 2.136 and 1.408 Å observed for Cr^0-$(C_6H_5CF_3)_2$,[29a] 2.155 and 1.410 Å observed for Cr^0-$(C_6H_5CF_3)(p\text{-}C_6H_4Me_2)$[29b] at 163 K. Likewise the Cr–C, C–C, and Cr–C_6(ring) centroid distances in $[Cr^I(C_6H_5Me)_2][TCNQ]$ and $[Cr^I(C_6H_5Me)_2][TCNQ]_2$ are 2.151, 1.411, and 1.67 Å[14b] and 2.18, 1.40, and 1.67 Å,[14a] respectively.

$[TCNE]^{\bullet-}$ exists as eclipsed dimeric dianions, $[TCNE]_2^{2-}$, for both **1** and **2β**. **1** possesses two independent anions, each with mirror plane perpendicular to the central CC bond (Figure 1b). The C–C for both anions is 1.436 (5) Å. The C–CN and C≡N bonds range from 1.405 (5) to 1.423 (5) and 1.136 (6) to 1.145 (6) Å, respectively, and average 1.414 and 1.140 Å, respectively. The NC–C–CN, NC–C–C, and N≡C—C angles range from 118.3 (3) to 118.8 (3), 119.7 (3) to 120.6 (3), and 177.9 (4) to 179.1 (4)° and average 118.6, 120.2, and 178.4°, respectively.

The resolution of **2β** is of poorer quality. The C–C spacing is 1.445 (10) Å, while the C–CN and C≡N bonds range from 1.35 (2) to 1.48 (2) and 1.05 (2) to 1.14 (3) Å, respectively, and average 1.40 and 1.10 Å, respectively. The NC–C–CN, NC–C–C, and N≡C—C angles range from 132.6 (8) to 133.6 (8), 109.8 (7) to 116.5 (6), and 160 (2) to 163 (1)° and average 133, 114, and 162°, respectively.

The central C–C bonds in the eclipsed, centrosymmetric $[TCNE]_2^{2-}$ dimer in **1** are parallel to each other and separated by 2.904 Å; the other intradimer C···C distance is 3.240 Å. Relative to TCNE,[8b,20,30] the central C–C bond of the $[TCNE]_2^{2-}$ in **1** elongates by ca. 0.08 Å to 1.436 (5) Å and the C–CN shortens by 0.03 Å to 1.408 (5) Å, whereas the C≡N distance contracts by ca. 0.02 Å to 1.139 (5) Å. Each monomer in the $S = 0$ $[TCNE]_2^{2-}$ dimer in **1** is nonplanar but bent 10° via a b_{3u} out-of-plane vibration, Figure 2. This $[TCNE]_2^{2-}$ dimer with a similar interdimer separation of 2.90 Å has also been observed for the electron-transfer salt $[Fe(C_5H_4)_2(CH_2)_3][TCNE]$.[20]

A detailed discussion of the geometry of the anion for **2β** is inappropriate as the anion is not well resolved. Nonetheless, some comparisons can be made. Analogous to **1**, the $[TCNE]_2^{2-}$ dimer in **2β** is also nonplanar with a 5.8° bending out of the plane relative to the central carbons. The smaller distortion may result from the 0.19-Å longer interplanar separation of 3.09 Å compared to 2.90 Å found for **1**, Table V. The structural parameters are very similar to those reported for the $[TCNE]_2^{2-}$ ion in $[Fe(C_5H_4)_2$-$(CH_2)_3][TCNE]$,[20] and the metric parameters are compared with those reported for TCNE, $[TCNE]^{\bullet-}$, $[TCNE]_2^{2-}$, and $[TCNE]^{2-}$ in Table V.

(28) Kulen, E.; Jellinek, F. *J. Organomet. Chem.* **1966**, *5*, 490.
(29) (a) Larson, S. B.; Seymour, C. M.; Lagowski, J. J. *Acta Crystallogr.* **1987**, *C43*, 1624–1626, (b) 1626–1628.
(30) Becker, P.; Coppens, P.; Ross, R. K. *J. Am. Chem. Soc.* **1973**, *95*, 7604.

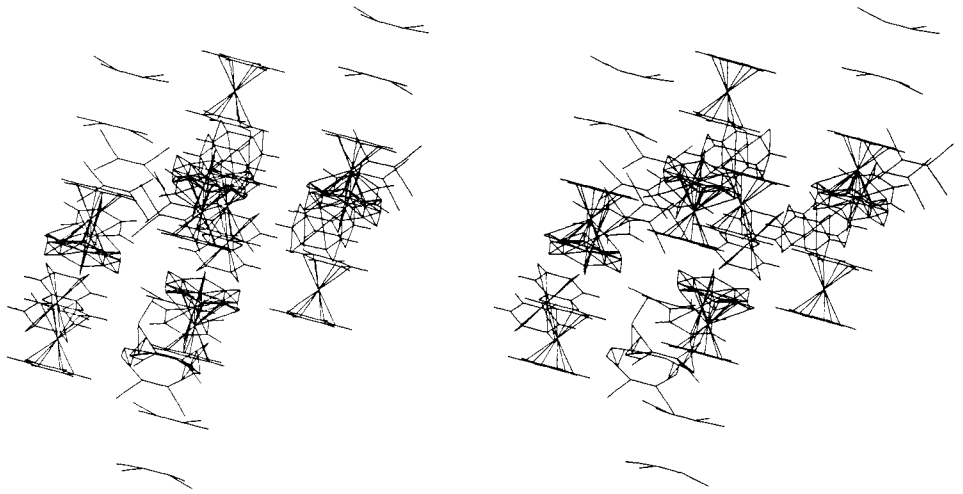

Figure 2. Stereoview of the unit cell for $[Cr(C_6H_6)_2][TCNE]$, **1**.

Table V. Summary of Crystallographically Determined Bond Lengths and Angles and $\nu(C{\equiv}N)$ for TCNE, $[TCNE]^{\bullet-}$, $[TCNE]^{2-}$, and $[TCNE]_2^{2-}$

	TCNE[a]	$[TCNE]^{\bullet-}$[b]	$[TCNE]_2^{2-}$[c]	**1**	**2β**	$[TCNE]^{2-}$[d]
sym point group	D_{2h}	D_{2h}	D_{2h}	D_{2h}	D_{2h}	D_{2d}
temp, °C		−30	−120	23	23	−50
C–C, Å	1.355 (2)	1.392 (9)	1.35 (2)	1.436 (5)	1.45	1.49 (2)
C–CN, Å	1.432 (1)	1.417 (2)	1.46	1.408 (5)	1.40	1.392 (8)
C≡N, Å	1.160 (1)	1.140 (4)	1.13	1.139 (5)	1.10	1.166 (3)
C—C≡N, deg	177.93 (7)	179.9	175.0	178.4 (4)	162.0	177.6
NC–C–CN, deg	116.11 (8)	117.7	118.5	118.6	133.0	117.1
C–C–CN, deg			120.0	120.2	114.0	
dev out of plane, deg	0	0	7.76	10.7	5.8	
R_w, %	3.4	5.4	13.1	4.4	8.1	8.3
dimer separation			2.90	2.90	3.09	
$\nu(C{\equiv}N)$, cm^{-1}	2221	2044	2161	2159		2069
	2259	2083	2168	2170		2140
			2191	2189		
ref	30	8b	21	this work	this work	30

[a] Neutron diffraction. [b] $[Fe(C_5Me_5)_2]^+$ salt. [c] $[Fe(C_5H_4)_2(CH_2)_3]_2^{\bullet+}$ salt. [d] $[Co(C_5Me_5)_2]^+$ salt.

Solid-State Structure. Unlike the structures found for the $[Fe(C_5Me_5)_2]^{\bullet+}$ salts of $[TCNE]^{\bullet-}$, $[DDQ]^{\bullet-}$, $[TCNQ]^{\bullet-}$, $[C_4(CN)_6]^{\bullet-}$, and $[C_6(CN)_6]^{\bullet-}$,[5b] compounds **1** and **2β** crystallize as a one-dimensional electron-transfer salt with dimer dianions sandwiched between two adjacent $[Cr(C_6H_6)_2]^{\bullet+}$ cations in a $\cdots D^+D^+A_2^{2-}D^+D^+\cdots$ one-dimensional arrangement. Since magnetic phenomena involve interchain as well as the intrachain interactions, it is important to discuss the inter- and intrachain Cr–Cr, Cr–N, and N–N separations. A stereoview of **1** is shown in Figure 2.

$[Cr(C_6H_6)_2][TCNE]$, 1. The unit cell is comprised of three unique interchain interactions, namely, A–B, A–D, and B–D, Figure 3. Chains A–C are essentially in-registry, whereas chains A–B and A–D are out-of-registry, Figure 4. The solid consists of parallel chains separated by 6.161, 6.534, and 7.480 Å with intrachain Cr···Cr separations of 6.702 and 13.264 Å. The interchain Cr···Cr distances are 6.305, 7.483, 7.948, 8.307, 9.911, and 10.434 Å. These distances are too great for strong spin–spin interaction not mediated by a radical.

$[Cr(C_6Me_3H_3)_2][TCNE]$, 2β. The unit cell is comprised of three unique interchain interactions, namely, E–F, E–G, and E–H, Figure S3 (supplementary material). Chains E–G are essentially in-registry, whereas chains E–F and E–H are out-of-registry, Figure S4. The solid consists of parallel chains separated by 7.686 and 8.099 Å with a longer interaction at 12.282 Å. The intrachain Cr···Cr separations are 6.932 and 13.602 Å. The interchain Cr···Cr distances are 8.429, 8.809, 8.998, 9.364, 11.427, 11.682, and 12.282 Å. These distances are also too great for strong spin–spin interaction not mediated by a radical.

Spectroscopic Properties

Vibrational Spectroscopy. The C≡N stretching bands in the infrared spectrum occur at 2144 and 2183 cm^{-1} for the $[Fe(C_5Me_5)_2]^{\bullet+}[TCNE]^{\bullet-}$ and $[Co(C_5Me_5)_2]^+[TCNE]^{\bullet-}$ salts.[8b,31]

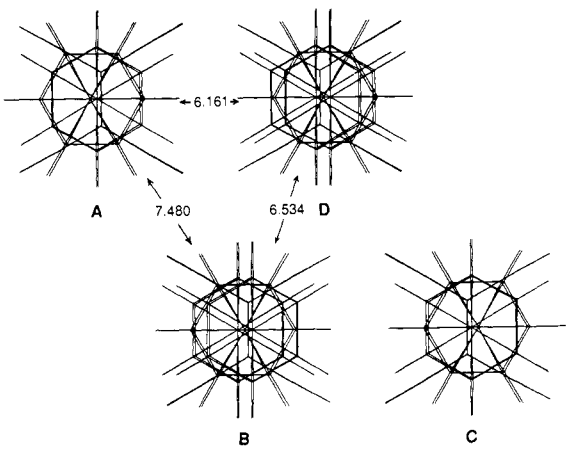

Figure 3. View normal to chains showing the four unique chains: A, B, C, and D for $[Cr(C_6H_6)_2][TCNE]$.

For **1** crystallized from acetonitrile we observe three strong C≡N stretching vibrations in the infrared region at 2159 s, 2170 s, and 2189 m cm^{-1}. The position of the bands indicates that the anion is monoreduced, but the lowering of the symmetry by an out-of-plane deformation as revealed by the X-ray diffraction is consistent with the observation of three infrared active bands rather than two for $[TCNE]^{\bullet-}$ isolated anions at 2144 s and 2183 m cm^{-1}.[31] The $\nu(C{\equiv}N)$ (Nujol) absorptions for the $[TCNE]_2^{2-}$ dimer in the complex $[Fe(C_5H_4)_2(CH_2)_3][TCNE]$ are 2161 s, 2169 s, and 2191 m cm^{-1}.

(31) Miller, J. S.; Dixon, D. A. *Science* **1987**, *235*, 871–873.

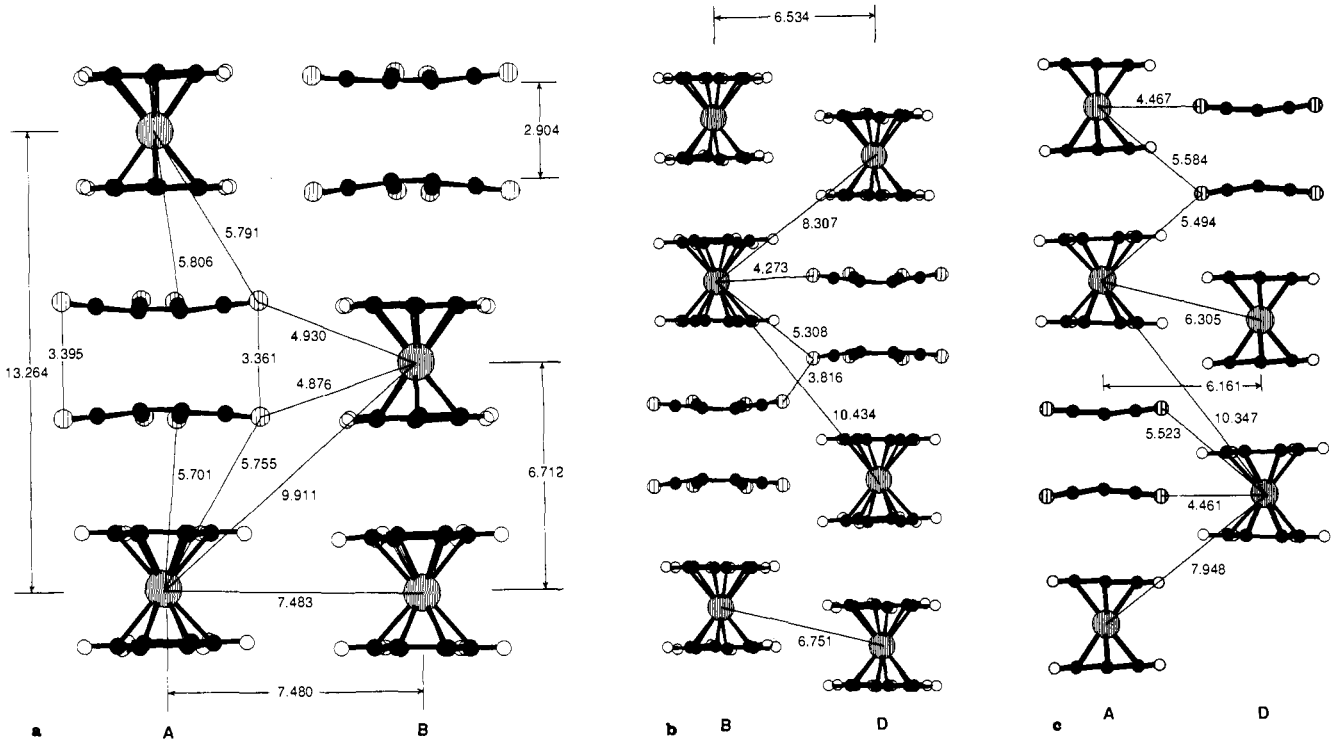

Figure 4. Interactions between chains A–B, A–D, and B–D.

The infrared spectra of either **2**α or **3** crystallized from THF show strong ν(C≡N) stretches at 2144 and 2183 cm^{-1}, which strongly indicates that crystallization from this solvent gives [TCNE]$^{\bullet-}$ and not [TCNE]$_2^{2-}$.

Electron Paramagnetic Resonance. The EPR spectra of [Cr(η-arene)$_2$]$^{\bullet+}$ as the [PF$_6$]$^-$ salts are typical with g = 1.987.[21] The room-temperature EPR spectrum of **1** in 2:1 THF:CH$_3$CN solution shows two isotropic signals with g = 2.001 (ΔH_{pp} = 7.3 G) and 1.986 (ΔH_{pp} = 14.4 G), each of equal intensity, Figure 5, which are assigned to [TCNE]$^{\bullet-}$ anion and [Cr(η-arene)$_2$]$^{\bullet+}$ cations, respectively. Similar results are observed for **2**α and **3**. In the solid state, **3** has only a broad peak ($\Delta H_{pp} \sim$ 600 G) at g = 1.984.

Magnetic Susceptibility. The 2–320 K Faraday balance susceptibility[32] shows that **1**, **2**α, **3**, and [Fe(C$_5$H$_4$)$_2$(CH$_2$)$_3$][TCNE] can be fit by the Curie–Weiss law, $\chi_M = C/(T - \theta)$. The structurally characterized complexes containing [TCNE]$_2^{2-}$ dimers, i.e., **1** and [Fe(C$_5$H$_4$)$_2$(CH$_2$)$_3$][TCNE], exhibit effective moments, μ_{eff}, of 1.70 and 2.51 μ_B and θ = −0.5 and −2 K, respectively. The value of μ_{eff} indicates that only the one $S = {}^1/_2$ radical per formula unit is contributing to the susceptibility. This is consistent with the structures possessing S = 0 [TCNE]$_2^{2-}$; i.e., only the radical cations contribute to the magnetic susceptibility. Previously, the magnetic susceptibilities of [Cr^I(C$_6$H$_6$)$_2$]$^{\bullet+}$I^{-}[33] (μ_{eff} of 1.72 μ_B and θ = −4.6 K), [Cr^I(C$_6$H$_5$CH$_3$)$_2$]$^{\bullet+}$I^{-}[33] (μ_{eff} of 1.72 μ_B and θ = −2.0 K), and [Cr^I(C$_6$H$_5$CH$_3$)$_2$]$^{\bullet+}$[AlCl$_4$]$^-$[19a] (μ_{eff} of 1.77 μ_B) have been reported. The linearity of the χ^{-1} vs T plot, Figure 6, argues that the singlet–triplet energy gap for [TCNE]$_2^{2-}$ must be sufficiently large so that there is no detectable triplet concentration at temperatures up to 320 K. The greater effective moment for [Fe(C$_5$H$_4$)$_2$(CH$_2$)$_3$]$^{\bullet+}$ is due to orientational effects as $g_\parallel$ = 3.86 and $g_\perp$ = 1.81,[34] and the moment is similar to the values found for ferrocenium salts of diamagnetic anions. Thus, the [TCNE]$_2^{2-}$ acts as a diamagnetic spacer between the radical cations and prevents the onset of cooperative magnetic ordering at low temperatures.

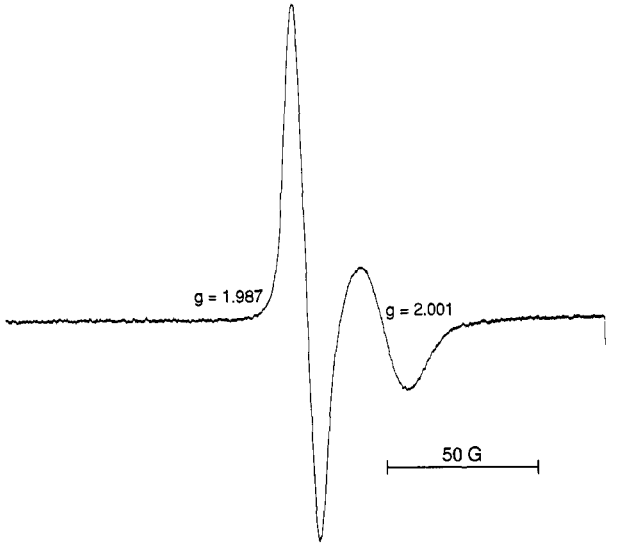

Figure 5. Solution (2:1 THF:MeCN) EPR spectrum of **1** at room temperature.

In contrast, **2**α and **3** exhibit different magnetic behavior, Figure 6, which shows least-squares fit of χ_M^{-1} vs T for **2**α and **3** to the Curie–Weiss law, $\chi_M = C/(T - \theta)$, between 50 and 300 K with a ferromagnetic θ of +11.0 (μ_{eff} = 2.44 μ_B) and 11.8 K (μ_{eff} = 2.37 μ_B), respectively. The magnetic moment is in good agreement for the value expected for two independent doublets, i.e., 2.45 μ_B. That is, each cation and anion have a spin.

Below ~5 K, the reciprocal susceptibility deviates from the Curie–Weiss law, and the molar susceptibilities of **2**α and **3** exhibit a marked field dependence, Figure 7. Enhancement of the low-temperature field dependence of the magnetization, $M(H)$, and low-field susceptibility is demonstrated by comparison with $M(H)$ obtained from the Brillouin function appropriate for independent $S = {}^1/_2$ spins. Thus

$$M = \sum N_i g_i J \tanh (x_i)$$

where

$$x_i = \mu_{B_i} H/k_B T = g_i J_b H/k_B T$$

(32) Diamagnetic corrections [Cr(C$_6$H$_6$)$_2$][TCNE] = −198 × 10^{-6} emu/mol, [Cr(C$_6$Me$_3$H$_3$)$_2$][TCNE] = −251 × 10^{-6} emu/mol, [Cr(C$_6$Me$_6$)$_2$][TCNE] = −318 × 10^{-6} emu/mol.

(33) Karimov, Yu. S.; Chibrikin, V. M.; Shchegolev, I. F. *J. Phys. Chem. Sol.* **1963**, *24*, 1683–1686.

(34) Duggan, D. M.; Hendrickson, D. N. *Inorg. Chem.* **1975**, *14*, 955–970.

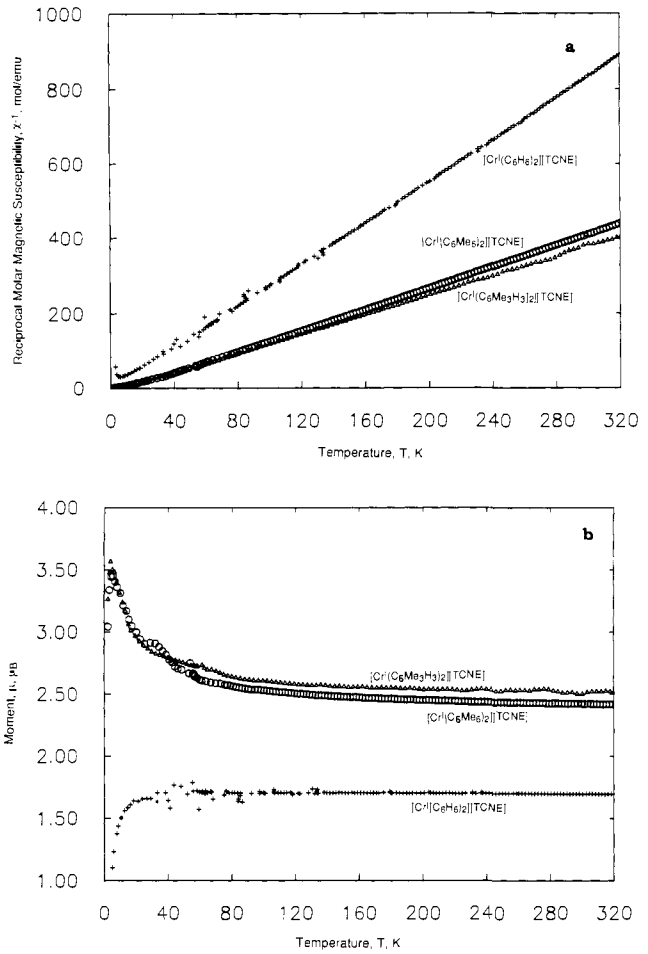

Figure 6. Inverse molar magnetic susceptibility (a) and moment (b) as function of temperature for **1**, **2**β, and **3**.

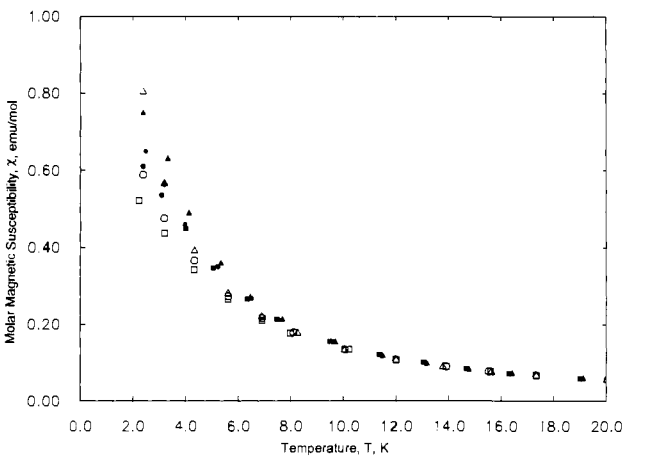

Figure 7. Field dependence of the magnetic susceptibility for [Cr($C_6Me_3H_3$)$_2$][TCNE], **2**β, and [Cr(C_6Me_6)$_2$][TCNE], **3** (△, ▲ = 5.2 kG; ○, ● = 15.8 kG; □, ■ 19.5 kG.

and N_i, g_i, and μ_i refer to the mole fraction, Lande g factor {g = 2 values for $[TCNE]^{\bullet-}$ [36] and $[Cr(C_6Me_6)_2]^{\bullet+}$ [21]}, and magnetic moment of each of spin site i. The magnetization saturates at 11 000 emu G/mol, as expected by eq 1 for two $g = 2.0$, $S = {}^1/_2$

$$M_s = NS\mu_B\Sigma g_i \quad (1)$$

radicals, though the approach to saturation with increasing field is more rapid, reflecting ferromagnetic coupling among the spins. There is no evidence of 3-D ordering of spins (bulk ferromagnetic behavior).[5] For example, hysteresis loops are not observed. Enhancement of $M(H)$ and $\chi(T)$ beyond the independent spin model can be parametrized by using the exact solution of the

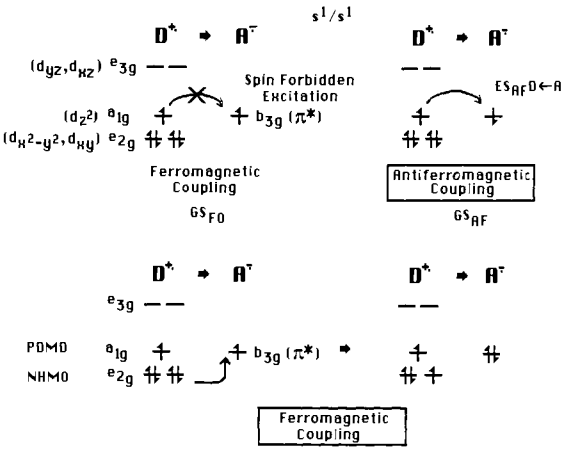

Figure 8. Stabilization of ferromagnetic coupling via retro-charge-transfer from a s^1 $[A]^{\bullet-}$ to d^3 $[D]^{\bullet+}$. Antiferromagnetically (singlet) coupled paramagnetic ground state arising from POMO A ← D charge transfer (top). Ferromagnetically (triplet) coupled paramagnetic ground state and stabilization of ferromagnetic coupling via arising from NHOMO A ← D charge transfer (bottom).

classical $S = {}^1/_2$ 1-D Ising model. Though an excellent parametrization of $\chi(T)$ and $M(H)$ in eq 2 is obtained for $J = +2.4$ K,

$$M(J,H,T) = \frac{\exp(J/k_BT)\sinh(H/k_BT)}{[\exp(2J/k_BT)\sinh^2(H/k_BT) + \exp(-2J/k_BT)]^{1/2}} \quad (2)$$

the Ising model is physically inappropriate. Neither quantum effects nor the presence of an isotropic g have been accounted for. This implies that the Heisenberg model may be more appropriate; however, a exact solution in a closed form for $\chi(T)$ and $M(H)$ does not exist.

Conclusion

The $\{[Cr^I(C_6Me_xH_{6-x})_2]^{\bullet+}\}_2[TCNE]_2^{2-}$ [x = 0, 3 (**2**β)] complexes possess linear $\cdots D^{\bullet+}D^{\bullet+}(AA)^{2-}D^{\bullet+}D^{\bullet+}(AA)^{2-}\cdots$ chains and do not exhibit cooperative magnetic behavior in the solid state. The observed independent spin magnetic properties are consistent with an unpaired electron per cation separated by a diamagnetic $[TCNE]_2^{2-}$ counterion. In contrast the susceptibilities of the $[Cr^I(C_6Me_xH_{6-x})_2]^{\bullet+}[TCNE]^{\bullet-}$ [x = 3 (**2**α), 6] salts are consistent with two unpaired electrons per formula unit and exhibit dominant ferromagnetic coupling as evidenced from a fit of the high-temperature susceptibility to the Curie–Weiss expression with $\theta = \approx +11.4$ K. Crystals suitable for single-crystal X-ray analysis, however, have not been prepared; thus, the structures of these salts are unknown. With the observation of ferromagnetic coupling in other electron-transfer salts with $\cdots D^{\bullet+}A^{\bullet-}D^{\bullet+}A^{\bullet-}D^{\bullet+}A^{\bullet-}\cdots$ linear chains[5] and the infrared evidence for isolated $[TCNE]^{\bullet-}$ and not $[TCNE]_2^{2-}$, we propose that these ferromagnetically coupled complexes also have this structural arrangement. Specific details of the intra- and interchain interactions arising from the canting and interchain registry of the chains as well as the interatomic separations must await the structural determinations.

A motivation for this study was to probe the effect of the electronic structure on the magnetic behavior. As was discussed earlier, the present understanding of the mechanism for stabilization of ferromagnetic coupling in molecular-based donor/acceptor complexes is configurational mixing of a charge-transfer excited state with the ground state.[5,16,17] The model predicts that for excitation from the HOMO of a donor to an acceptor both with a half-filled nondegenerate HOMO, as is the case for these $[TCNE]^{\bullet-}$ salts, only antiferromagnetic coupling is stabilized. Since the $[Cr(arene)_2]^{\bullet+}$ cation has an $e_g^4a_{1g}^1$ electronic structure and an $^2A_{1g}$ ground state,[18,35,36] antiferromagnetic behavior is

(35) Reiger, P. H.; Bernal, I.; Fraenkel, G. K. *J. Am. Chem. Soc.* **1961**, *83*, 3918.
(36) Osborne, J. H.; Trogler, W. C.; Morand, P. C.; Francis, C. G. *Organometallics* **1987**, *6*, 94–100.

predicted. The observed ferromagnetic coupling thus suggests that the model is inadequate. The model, however, is consistent with the observed data if we consider that the acceptor ← donor charge-transfer excitation results from the next highest occupied molecular orbital (NHOMO), not the POMO of the cation, to the radical anion POMO, Figure 8. Thus, ferromagnetic coupling which may ultimately lead to bulk ferromagnetic behavior as noted for $[Fe(C_5Me_5)_2]^{+}[TCNE]^{-}$ [5,8,9] is achievable for systems where both the donor and acceptor have ^2A_g ground states and may be useful for understanding the ferromagnetic coupling reported for galvinoxyl[37] and $[TTF]^{+}\{M[S_2C_2(CF_3)_2]_2\}^{-}$ (TTF = tetrathiofulvalene; M = Pt, Ni).[38] Computational studies involving the charge-transfer integral for various ^2A and ^2E ground-state donor and acceptors as a function of different geometries are in progress.

(37) Agawa, K.; Sugano, T.; Kinoshita, M. *J. Chem. Phys.* **1986**, *85*, 2211-2223. Agawa, K.; Sugano, T.; Kinoshita, M. *Chem. Phys. Lett.* **1987**, *141*, 540-544.

(38) Jacobs, I. S.; Hart, H. R., Jr.; Interrante, L. V.; Bray, J. W.; Kaspar, J. S.; Watkins, G. D.; Prober, D. E.; Wolf, W. P.; Bonner, J. C. *Physica (Amsterdam)* **1977**, *86-88B*, 655-656.

Acknowledgment. A.C., A.J.E., and J.S.M. gratefully acknowledge support from the Department of Energy Division of Materials Science Grant No. DE-FG02-86ER45271.A000. We also appreciate the synthetic assistance supplied by C. Vazquez and D. Wipf as well as the Faraday susceptibility data taken by R. S. McLean and EPR spectra taken by S. Hill and P. J. Krusic (Dupont CR&DD).

Registry No. 1, 98397-77-4; **2α**, 122144-56-3; **2β**, 122144-58-5; **3**, 122144-57-4.

Supplementary Material Available: Tables of fractional coordinates/anisotropic thermal parameters, general temperature factors, and cation bond angles $[Cr^{I}(C_6Me_xH_{6-x})_2][TCNE]$ (x = 0, 3), figures of the atom labeling, stereoviews, and solid-state interactions, and tables of the bond distances, anion bond angles, and least-squares plane for **2β** (27 pages); listing of observed and calculated structure factors for $[Cr^{I}(C_6Me_xH_{6-x})_2][TCNE]$ (19 pages). Ordering information is given on any current masthead page.

Hydrolysis of Toxic Organophosphorus Compounds by *o*-Iodosobenzoic Acid and Its Derivatives

Philip S. Hammond,*,† Jeffry S. Forster,† Claire N. Lieske,† and H. Dupont Durst‡

Contribution from the U.S. Army Medical Research Institute of Chemical Defense and The Chemical Research, Development and Engineering Center, Aberdeen Proving Ground, Maryland 21010-5425. *Received November 2, 1988. Revised Manuscript Received May 22, 1989*

Abstract: The 1,2,2-trimethylpropyl and the 1-methylethyl esters of methylphosphonofluoridic acid (soman and sarin, respectively), ethyl *N*,*N*-dimethylphosphoramidocyanidate (tabun), and the diethyl 4-nitrophenyl ester of phosphoric acid (paraoxon) are hydrolyzed effectively in aqueous micellar cetyltrimethylammonium chloride (CTAC) solutions at pH 7.5 in the presence of the deprotonated form of *o*-iodosobenzoic acid (**5a**), 5-(*n*-octyloxy)-2-iodosobenzoate (**5b**), or 5-nitro-2-iodosobenzoate (**5d**). Aqueous CTAC solutions (1×10^{-2} M) containing 7.5×10^{-4} M **5a** hydrolyze 1×10^{-3} M soman with a half-life of approximately 15 s, $k_{obs} = 0.046$ s^{-1}, at 25 °C. Under similar conditions but with **5a** at 1×10^{-4} M, hydrolysis rates for both sarin and tabun were slower than that for soman, i.e., $k_{obs} = 2.35 \times 10^{-3}$ and 1.99×10^{-3} s^{-1}, respectively, while the k_{obs} for soman hydrolysis was equal to 8.08×10^{-3} s^{-1}. Reactions with soman, sarin, and paraoxon appear to be truly catalytic, while tabun hydrolysis may be more complicated. The 5-(*n*-octyloxy) derivative of *o*-iodosobenzoic acid (**5b**) gave rates with soman and sarin 2-3 times greater than those for the parent compound (**5a**). Derivative **5d** showed approximately 50% the activity of the parent compound for these same substrates. Similar rates of hydrolysis were found when either CTAC or cetylpyridinium chloride (CPC) was used as surfactants with **5a** as catalyst. Activity is not limited to a micellar environment. Both **5a** and **5b** promote the hydrolysis of organophosphorus compounds at pH 8.2 (bicarbonate buffer) in the absence of a surfactant and show even greater activity when ionically exchanged onto an ion exchange resin.

The facile hydrolysis of toxic organophosphorus compounds is of theoretical and practical interest since these compounds appear in day-to-day applications as pesticides and have been used as potent chemical warfare agents. Over the past decade, a number of approaches have been used to address the problem of hydrolysis/detoxification of such compounds. These include reactions of various organophosphorus esters with surface active oximes[1] or oximates in micellar solutions[2] and enzyme-catalyzed hydrolysis,[3] as well as reactions with aqueous sodium perborate,[4a] water-soluble *N*-bromooxazolidinones,[4b] and β-cyclodextrin (cycloheptaamylose) or related compounds.[5]

Many investigators have examined the reactivity of both carboxylic and organophosphorus esters in organized assemblies such as vesicles, micelles, and aggregates of various reagents.[6] For example, Menger examined the hydrolysis of *p*-nitrophenyl diphenyl phosphate (**1a**, PNPDPP) by a functionalized surfactant

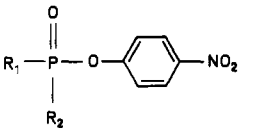

1a (PNPDPP), $R_1 = R_2 = C_6H_5O$
1b (PNPDEP), $R_1 = R_2 = C_2H_5O$
1c (PNPIMP), $R_1 = i\text{-}C_4H_9O$; $R_2 = CH_3$
1d (PNPIPP), $R_1 = i\text{-}C_3H_7$; $R_2 = C_6H_5$

containing a hydrated aldehyde terminus (**2**) and has shown this reagent to provide catalytic turnover of that substrate.[7a] In more

†U.S. Army Medical Research Institute of Chemical Defense.
‡The Chemical Research, Development and Engineering Center.

(1) Rossman, K. *Proceedings of the International Symposium on Protection Against Chemical Warfare Agents*, Stockholm, Sweden, June 6-9, 1983; p 233.

(2) Epstein, J.; Kaminski, J. J.; Bodor, N.; Enever, R.; Sowa, J.; Higuchi, T. *J. Org. Chem.* **1978**, *43*, 2816.

(3) Hoskin, F. C. G.; Kirkish, M. A.; Steinmann, K. E. *Fund. Appl. Toxicol.* **1984**, *4*, S165.